BEILSTEIN JOURNAL OF NANOTECHNOLOGY

Angstrom-scale flatness using selective nanoscale etching

Takashi Yatsui*[1], Hiroshi Saito[1] and Katsuyuki Nobusada[2]

Full Research Paper

Open Access

Address:
[1]School of Engineering, University of Tokyo, Bunkyo-ku, Tokyo, 113-8656 Japan and [2]Department of Theoretical and Computational Molecular Science, Institute for Molecular Science, Myodaiji, Okazaki 444-8585 Japan

Email:
Takashi Yatsui* - yatsui@ee.t.u-tokyo.ac.jp

* Corresponding author

Keywords:
Angstrom-scale flatness; optical near-field; wet etching

Beilstein J. Nanotechnol. **2017,** *8,* 2181–2185.
doi:10.3762/bjnano.8.217

Received: 07 June 2017
Accepted: 27 September 2017
Published: 18 October 2017

Associate Editor: A. J. Meixner

Abstract

The realization of flat surfaces on the angstrom scale is required in advanced devices to avoid loss due to carrier (electron and/or photon) scattering. In this work, we have developed a new surface flattening method that involves near-field etching, where optical near-fields (ONFs) act to dissociate the molecules. ONFs selectively generated at the apex of protrusions on the surface selectively etch the protrusions. To confirm the selective etching of the nanoscale structure, we compared near-field etching using both gas molecules and ions in liquid phase. Using two-dimensional Fourier analysis, we found that near-field etching is an effective way to etch on the scale of less than 10 nm for both wet and dry etching techniques. In addition, near-field dry etching may be effective for the selective etching of nanoscale structures with large mean free path values.

Introduction

The use of optical near-fields (ONFs) has contributed to the progress of nanoscale optical measurements [1], nanoscale fabrication [2], and photonic devices [3] below the diffraction limit of light. Recent ONF studies have exploited non-uniformity to realize new properties such as second harmonic generation [4], dipole-forbidden transitions [5], and indirect band transitions [6-8].

Because the ONF can achieve dipole-forbidden transitions, we can create selective chemical reactions that occur only where the ONF has been generated. Using this concept, we have developed a near-field etching technique. In this process, the molecules are dissociated by an ONF with a lower photon energy than that of the molecules (see Figure 1). When light irradiates the substrate, the ONF is generated only at the protrusions because of their non-uniformity. Subsequently, the molecules are dissociated by the ONF, and the dissociated radicals selectively etch the protrusions. Finally, the ONF disappears and the etching process stops automatically. Near-field etching is performed using Cl_2 gas for glass, GaN [9], and plastic surfaces, and O_2 gas for diamond and organic materials [10]. Atomically flat surfaces both on the flat regions and on three-dimensional structures has been achieved.

In this study, we compared near-field etching using a solution (wet etching) as well as dry etching. To evaluate the ONF effect

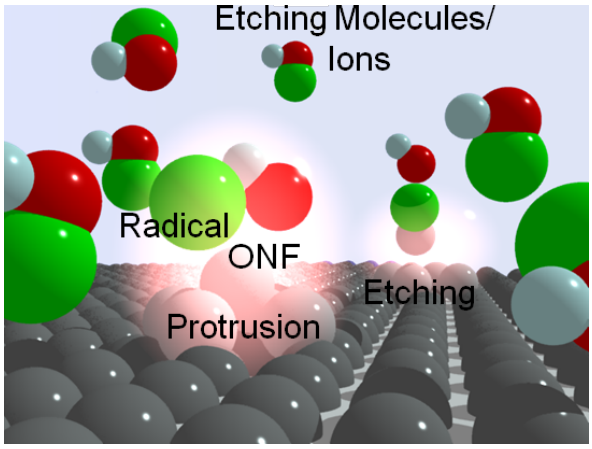

Figure 1: Schematic of the near-field etching process.

with respect to wet or dry etching, we examined the etching characteristics using a two-dimensional Fourier analysis.

Experimental

Nanoscale etching

For dry etching, we used Cl_2 gas at a pressure of 200 Pa. 25 wt % calcium hypochlorous acid ($Ca(ClO)_2$) was used as the source ion for wet etching. To dissociate the Cl_2 or hypochlorous acid, we used a continuous-wave diode-pumped solid-state (DPSS) laser (λ = 532 nm; 2.33 eV; excitation power: 119.4 W/cm^2). Thus, the incident photon energy was lower than the dissociation energy of Cl_2 (3.10 eV) [11] and the hypochlorous acid (3.35 eV) [12]; therefore, the Cl_2 or hypochlorous acid dissociated on the protrusions only. In the solution, a light source with a photon energy of 4.66 eV (higher than the dissociation energy) dissociated the hypochlorous acid and consequently produced Cl radicals [13]. This process is expected to be similar to the etching of glass when Cl_2 gas is used. The laser light was incident from the top of the substrate through a chamber with 200 Pa Cl_2 for dry etching or a drop of 10 µL $Ca(ClO)_2$ (25 wt %) for wet etching (see Figure 2). The absorption edge of fused silica is approximately 7.9 eV (157 nm) [14]; thus, we could exclude the effect of carrier generation in the fused silica. To evaluate the changes in the surface profiles, we used an atomic force microscope (AFM) with a "Sampling Intelligent Scan" mode (Hitachi-Hitech-Science Corp.). The scanning area of the AFM was 10 × 10 µm and 256 × 256 pixels.

Results and Discussion

Figure 3a–c shows the respective AFM images obtained 0 min, 5 min, and 35 min after wet etching. In the AFM images, the surface roughness (R_a) was found to be 0.161, 0.134, and 0.100 nm, respectively (solid circles in Figure 3d). In addition, we checked the R_a where light was not irradiated with the $Ca(ClO)_2$ solution and found that its value was unchanged (0.139 nm for before and 0.138 nm for after etching; solid squares in Figure 3d). These results indicate that near-field wet etching decreased the surface roughness. We also plotted the root mean square (RMS) roughness values in Figure 3d. Although the value is not the same, they have a similar time dependence as R_a.

To evaluate the etching properties, we calculated two-dimensional Fourier power spectra. Figure 4a–c shows the respective Fourier power spectra calculated from Figure 3a–c, respectively. To find the differences, the averaged cross-sectional profiles are plotted in Figure 4d. In addition, Figure 4e shows the ratio of the power spectra before etching to the power spectra after and before etching. A decrease in this ratio implies the etching was successful. These results show that at the beginning of the near-field wet etching, larger scale areas (more than 30 nm)

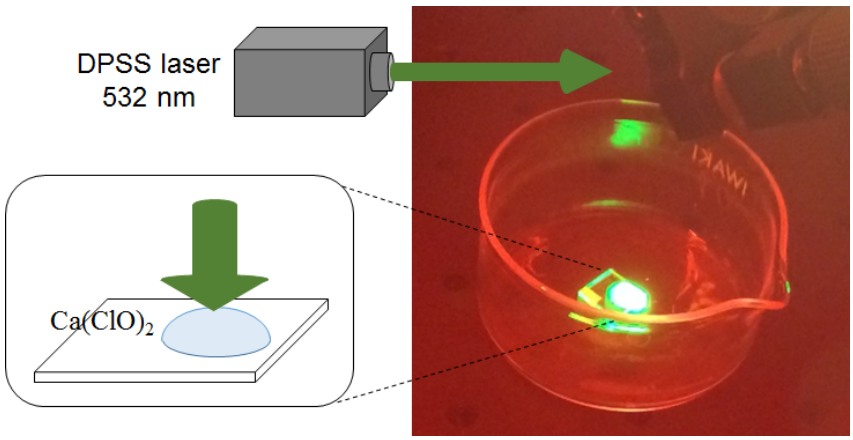

Figure 2: Experimental setup for the near-field wet etching technique.

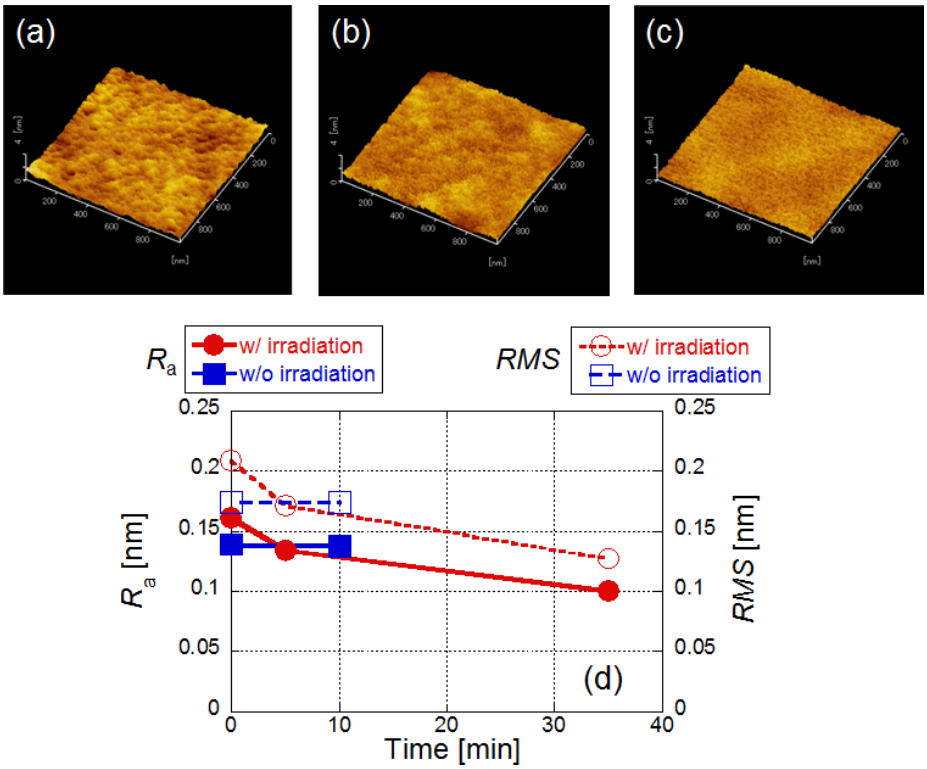

Figure 3: Time dependence of surface roughness using a solution (wet etchng). AFM images taken (a) before etching, (b) after 5 min, and (c) after 35 min. (d) Time dependence of the value of R_a. Red solid circles: with irradiation, blue solid squares: without irradiation. Time dependence of the value of RMS (right hand side). Red open circles: with irradiation, blue open squares: without irradiation.

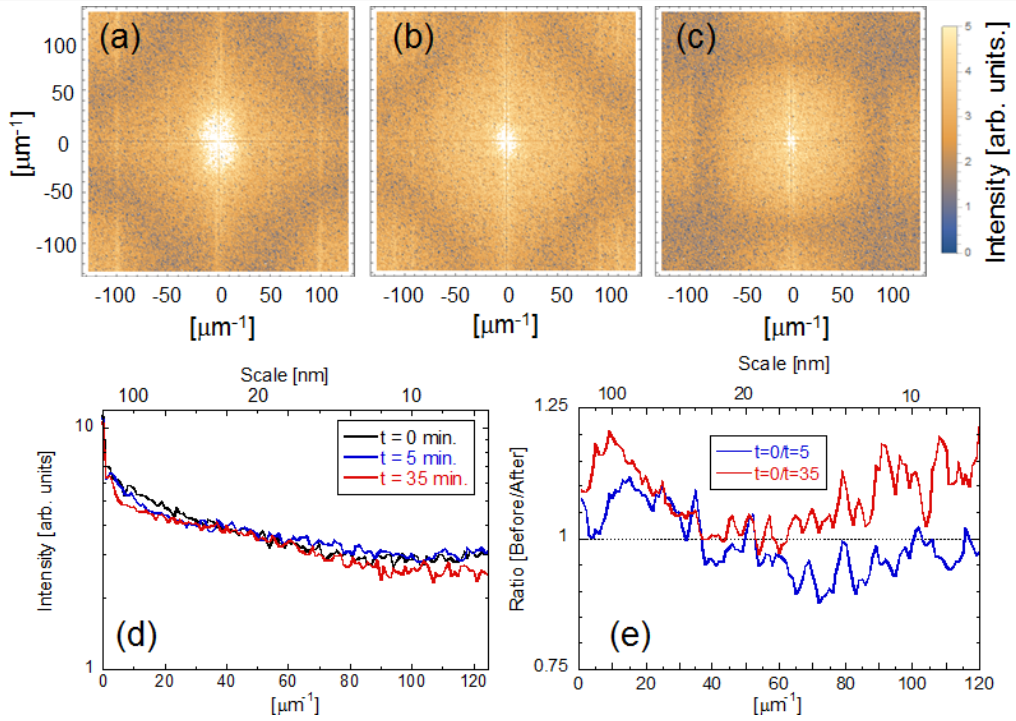

Figure 4: Time dependence of Fourier power spectra using a solution. Fourier power spectra taken (a) before etching, (b) after 5 min, and (c) after 35 min. (d) Averaged cross-sectional profiles. (e) Ratio of the power spectra before etching to the power spectra after etching. Blue solid line: before (t = 0 min)/after (t = 5 min), red solid line: before (t = 0 min)/after (t = 35 min).

were etched, and after that, smaller scale areas (less than 15 nm) were also etched.

We compared the etching properties obtained from these results with those from a near-field dry etching technique. For this purpose, we obtained AFM images before and after near-field etching using Cl_2 gas. Figure 5a,b shows images 0 min and 30 min after etching. The AFM images show that the R_a was reduced from 0.338 nm to 0.208 nm (solid triangles in Figure 5c). We plotted RMS values in Figure 5c and found a similar time dependence as with R_a. We obtained the two-dimensional Fourier power spectra from the AFM images. Figure 6a,b shows the respective power spectra before and after near-field etching using Cl_2. To find the differences, the averaged cross-sectional profiles are plotted in Figure 6c. In addition, Figure 6d shows the ratio of the power spectra before etching to the power spectra after etching (green solid line). In this figure, we also compare the same ratio for wet etching (red solid line) and without irradiation (solid black line). These results show that although the ratio did not change in the absence of irradiation, smaller scale areas less than 10 nm were also etched in the near-field dry etching process.

To understand the differences of the etching properties, we estimated the mean free paths (MFPs) of Cl_2 and ClO^-. The MFP of Cl_2 in the gas phase is on the order of 10 µm

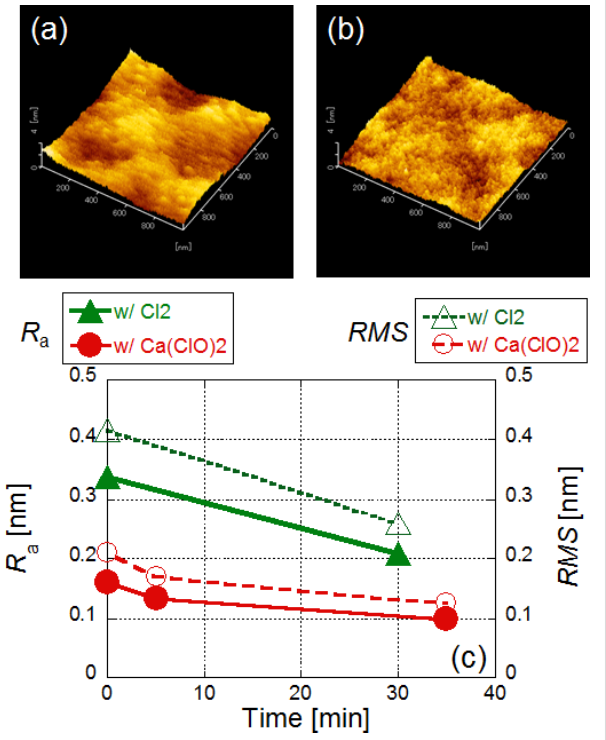

Figure 5: Time dependence of surface roughness. AFM images taken (a) before etching and (b) after 30 min. (c) Time dependence of the value of R_a. Red solid circles: with $Ca(ClO)_2$, green solid triangles: with Cl_2. Time dependence of the value of RMS. Red open circles: with $Ca(ClO)_2$, green open triangles: with Cl_2.

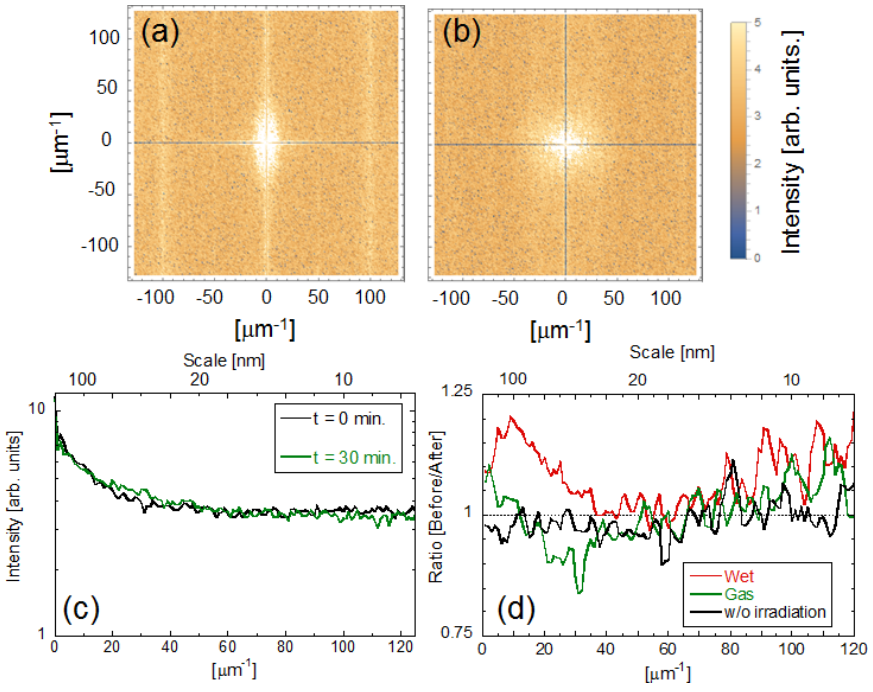

Figure 6: Time dependence of Fourier power spectra using a gas. Fourier power spectra taken (a) before etching and (b) after 30 min. (c) Averaged cross-sectional profiles. (d) Ratio of the power spectra before to the power spectra after etching. Red solid line: before (t = 0 min)/after (t = 35 min) etching using a solution, black solid line: before (t = 0 min)/after (t = 10 min) etching using a solution without irradiation, green solid line: before (t = 0 min)/after (t = 30 min) etching using a gas.

($\approx RT/\sqrt{2}N_A\pi d^2P$ [15], where R = 8.31 J $K^{-1}mol^{-1}$, T = 300 K, $N_A = 6.02 \times 10^{23}$ mol^{-1}, $d = 200 \times 10^{-12}$ m (the diameter of a Cl_2 molecule) and P = 200 Pa). In contrast, the MFP of ions in solution is on the order of 10 pm [16], which is 10^{-7} times smaller than that of Cl_2 gas. Such a low MFP value for ions in solution resulted in etching near the protrusions where the ions or molecules are dissociated. However, in the case of near-field dry etching, because of a greater MFP value of the gas phase that exceeds the scanning area, the dissociated atoms can react only when they are located at the protrusions where the ONF generated.

Conclusion

Using two-dimensional Fourier analysis, we found that near-field etching is effective for etching on smaller scales less than 10 nm for both wet and dry etching. In addition, by comparing wet and dry etching, near-field dry etching was shown to be effective for the selective etching of nanoscale structures because of the large value of the mean free path of the etching molecules. Hence, further control of the selective etching at smaller scales should be achievable by controlling mean free path (i.e. the partial pressure of the gas).

Acknowledgements

The authors wish to express special thanks to Mr. Maiku Yamaguchi (University of Tokyo) for active support and discussion. We thank Mrs. Etsuko Ota (University of Tokyo) for the AFM measurements. This work was partially supported by a MEXT Grant-in-Aid for Scientific Research (B) (No. 26286022), a MEXT Grant-in-Aid for Scientific Research (A) (No. 17H01262), a MEXT Grant-in-Aid for Challenging Research (Exploratory) (No. 17K20091), a MEXT Nanotechnology Platform (No.12024046), Japan (JSPS)-Korea (NRF) Bilateral Program, Japan (JSPS)-France (MAEDI) Bilateral Program, the JSPS Core-to-Core Program (A. Advanced Research Networks), Nippon Sheet Glass Foundation for Materials Science and Engineering, Iketani Science and Technology Foundation, Asahi Glass Foundation, the Yazaki Memorial Foundation, and the Research Foundation for Opto-Science and Technology. The author contributions are as follows: T.Y. planned the project. H.S. performed the experiments and Fourier analysis. All authors discussed the results. K.N. and T.Y. wrote the manuscript and edited the final manuscript. All authors reviewed the manuscript.

References

1. Betzig, E.; Chichester, R. J. *Science* **1993,** *262,* 1422–1425. doi:10.1126/science.262.5138.1422
2. Fang, N.; Lee, H.; Sun, C.; Zhang, X. *Science* **2005,** *308,* 534–537. doi:10.1126/science.1108759
3. Yatsui, T.; Sangu, S.; Kawazoe, T.; Ohtsu, M.; An, S. J.; Yoo, J.; Yi, G.-C. *Appl. Phys. Lett.* **2007,** *90,* 223110. doi:10.1063/1.2743949
4. Yamaguchi, M.; Nobusada, K.; Kawazoe, T.; Yatsui, T. *Appl. Phys. Lett.* **2015,** *106,* 191103. doi:10.1063/1.4921005
5. Yamaguchi, M.; Nobusada, K. *Phys. Rev. A* **2016,** *93,* 023416. doi:10.1103/PhysRevA.93.023416
6. Kirkengen, M.; Bergli, J.; Galperin, Y. M. *J. Appl. Phys.* **2007,** *102,* 093713. doi:10.1063/1.2809368
7. Jung, J.; Trolle, M. L.; Pedersen, K.; Pedersen, T. G. *Phys. Rev. B* **2011,** *84,* 165447. doi:10.1103/PhysRevB.84.165447
8. Yamaguchi, M.; Nobusada, K. *Phys. Rev. B* **2016,** *93,* 195111. doi:10.1103/PhysRevB.93.195111
9. Yatsui, T.; Nomura, W.; Stehlin, F.; Soppera, O.; Naruse, M.; Ohtsu, M. *Beilstein J. Nanotechnol.* **2013,** *4,* 875–885. doi:10.3762/bjnano.4.99
10. Yatsui, T.; Tsuboi, T.; Yamaguchi, M.; Nobusada, K.; Tojo, S.; Stehlin, F.; Soppera, O.; Bloch, D. *Light: Sci. Appl.* **2016,** *5,* e16054. doi:10.1038/lsa.2016.54
11. Kullmer, R.; Bäuerle, D. *Appl. Phys. A* **1987,** *43,* 227–232. doi:10.1007/BF00615982
12. Nakagawara, S.; Goto, T.; Nara, M.; Ozawa, Y.; Hotta, K.; Arata, Y. *Anal. Sci.* **1998,** *14,* 691–698. doi:10.2116/analsci.14.691
13. Thomsen, C. L.; Madsen, D.; Poulsen, J. A.; Thøgersen, J.; Knak Jensen, S. J. *J. Chem. Phys.* **2001,** *115,* 9361–9369. doi:10.1063/1.1413964
14. Saito, K.; Ikushima, A. J. *Phys. Rev. B* **2000,** *62,* 8584–8587. doi:10.1103/PhysRevB.62.8584
15. Atkins, P.; de Paula, J. *Atkins' Physical Chemistry;* Oxford University Press: Oxford, U.K., 2010.
16. Chinen, H.; Mawatari, K.; Pihosh, Y.; Morikawa, K.; Kazoe, Y.; Tsukahara, T.; Kitamori, T. *Angew. Chem., Int. Ed.* **2012,** *51,* 3573–3577. doi:10.1002/anie.201104883

License and Terms